In Silico Mutation of Cysteine Residues in the Ligand-Binding Domain of an *N*-Methyl-D-aspartate Receptor†

Samantha L. Kaye, Mark S. P. Sansom, and Philip C. Biggin*

Structural Bioinformatics and Computational Biochemistry, Department of Biochemistry, The University of Oxford, South Parks Road, Oxford OX1 3QU, U.K.

Received July 19, 2006; Revised Manuscript Received December 19, 2006

ABSTRACT: The precise nature of redox modulation of *N*-methyl-D-aspartate (NMDA) receptors is still unclear, although it is thought to be related to the formation and breaking of disulfide bonds. Recent structural data demonstrated the way in which disulfide bonds in the ligand-binding core of the NR1 subunit are arranged. However, the structures were not able to reconcile existing experimental data that examined the effects of mutating these cysteine residues. We have used molecular dynamics (MD) simulations of a series of in silico mutations to try and address this in terms of the current structure of the NR1 ligand-binding domain. A double mutation that removes the disulfide bridge between C744 and C798 gives rise to greater interlobe mobility which was predicted from the crystal structure information but, unexpectedly, also appears to predispose the receptor toward greater flexibility in the hinge region. Removal of the disulfide bond between C454 and C420 did not show any appreciable difference from the "wild-type" simulation, suggesting that removal of this would not change receptor properties, which is in agreement with experimental findings. Furthermore, the position of the C454 side chain could be characterized into discrete rotamers, which may reflect the observation of alternative density in the crystal structure for this residue. Simulations in which two of the disulfide bonds are removed via mutations to alanine (C420A and C436A) resulted in a tendency of the protein to adopt a partially closed conformation.

Glutamate is an important neurotransmitter that is required for fast synaptic neurotransmission. The ionotropic glutamate receptors (iGluRs)[1] are ligand-gated ion channels that can be classified into three major families according to their pharmacology: amino-3-hydroxy-5-methyl-4-isoxazolepropionic acid (AMPA), kainate, and *N*-methyl-D-aspartate (NMDA). Glutamate is, however, the relevant agonist in vivo (*1*). NMDA receptors are distinct from AMPA and kainate receptors in that they require both glutamate and glycine for activation and membrane depolarization, with glycine acting as a coagonist (*2*, *3*). It has also been suggested that D-serine might be the endogenous coagonist (*4*−*6*). The receptor is a heterotetrameric cation channel comprised of NR1 subunits which contain the glycine binding site along with NR2A-D subunits which contain glutamate-binding sites. Recent studies have indicated that NMDA receptors are comprised of two NR1 and two NR2 subunits arranged as a dimer of dimers (*7*, *8*). The heterogeneity of the complex is further extended if the third subtype (NR3) is also taken into account (*9*). Unlike AMPA and kainate receptors [where Ca^{2+} permeability is dictated by mRNA editing at the Q/R site (*10*)], NMDA receptors are always Ca^{2+} permeable. This calcium permeability is thought to underpin their role in long-term potentiation and learning processes in the brain (*11*). However, overstimulation can result in excessive Ca^{2+} influx into neurons leading to excitotoxic neuronal cell death associated with ischemia (*12*), head trauma (*13*), and other pathological conditions such as Parkinson's disease (*14*).

Each NMDA receptor subunit is comprised of an amino-terminal binding domain (ATD) which shows homology to the leucine-isoleucine-valine binding protein (LIVBP) protein (*15*), a ligand-binding domain (LBD), three transmembrane helices (M1, M2, and M3), a reentrant P-loop, and a carboxy-terminal domain (CTD) for which little structural information exists. The LBD is comprised of two discontinuous polypeptide chains, S1 and S2, that form two distinct lobes or subdomains, D1 and D2 (Figure 1A,B). An isolated S1S2 ligand-binding core has been shown to bind ligands with similar affinity as wild-type receptors (*16*, *17*).

NMDA receptors are also modulated in a variety of different ways including by protons (*18*), zinc (*19*), and redox agents (*20*), which are thought to act on the cysteine residues within both the ATD (*21*) and the LBD. Recently, crystal structures of the ligand-binding core of the NR1 (*16*, *17*) and NR2A (*22*) have been presented. The overall fold and structure are very similar to those observed for crystal structures of the ligand-binding domains for the (non-NMDA) GluR2 (*23*−*25*), GluR5 (*26*, *27*), and GluR6 receptors (*27*, *28*). For a recent review see ref *29*. The

† S.L.K. acknowledges the MRC for a studentship. M.S.P.S. and P.C.B. thank the Wellcome Trust for support.

* To whom correspondence should be addressed. E-mail: Philip.biggin@bioch.ox.ac.uk. Tel: +44 1865 275255. Fax: +44 1865 275273.

[1] Abbreviations: iGluR, ionotropic glutamate receptor; NMDA, *N*-methyl-D-aspartate; AMPA, amino-3-hydroxy-5-methyl-4-isoxazolepropionic acid; MD, molecular dynamics; ATD, amino-terminal domain; LBD, ligand-binding domain; CTD, carboxy-terminal domain; RMSD, root mean square deviation; RMSF, root mean square fluctuation; SPC, simple point charge (water model); NPT, constant number of particles (*N*), constant pressure (*P*), constant temperature (*T*) thermodynamic ensemble.

10.1021/bi061462d CCC: $37.00
Published on Web 02/01/2007

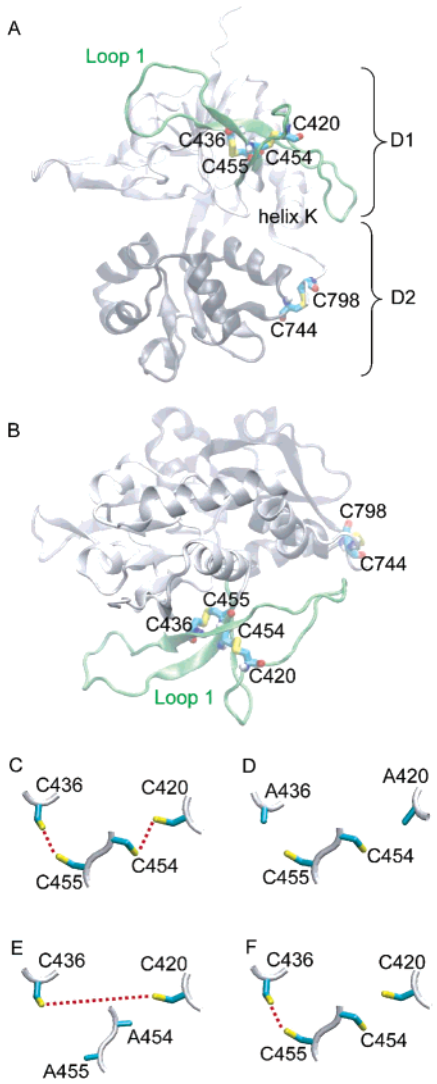

FIGURE 1: (A) shows a cartoon of the ligand-binding domain based upon the starting structure of the open-apo simulation. The D1 domain is colored light gray with loop 1 in green. The D2 domain is in dark gray. Cysteine residues proposed to form disulfide bridges are shown in licorice format. (B) as in (A) but rotated about the *x*-axis by approximately 90°. (C) schematically shows the disulfide bridge arrangement found in the crystal structures for the C436, C420, C454, and C455 residues. (D) Schematic of the mutations for the C420A-C436A simulation. (E) Schematic of the arrangement for the C454A-C455A simulation. (F) Schematic of the C454* simulation setup where the C436−C454 disulfide is maintained but the C420−C454 is not.

coupling of agonist binding to channel activation in glutamate receptors is not well understood, but various mechanisms have been proposed that fit the available data (*30*, *31*). Interestingly, despite the similarity in the ligand-binding cores, the coupling mechanism between the ligand-binding core and transmembrane channel domain appears to be different for NMDA and AMPA receptors. In the case of AMPA receptors, there is linear relationship between cleft opening and agonist efficacy, with full agonists inducing complete closure of the cleft and partial agonist inducing intermediate levels of cleft closure. In contrast, partial and full agonists for the NMDA receptor induce similar degrees of domain closure. For a discussion of this see ref *32*.

The NMDA X-ray structures reveal the position of several cysteine residues and suggest where disulfide bridges may exist. As with all known eukaryotic iGluR ligand-binding domain (LBD) structures, NR1 has a conserved disulfide bridge that tethers the C-terminal strand to domain D2 (Figure 1A,B). In NR1 the contributing residues are C744, which is located adjacent to helix I, and C798, adjacent to helix K. In 1994, Sullivan et al. (*33*) showed that performing a double mutation (C744A-C798A) leads to a 6-fold decrease in NMDA EC_{50}. Although the NR1 subunit binds glycine, the fold similarity (to NR2) and the possibility of allosteric cooperativity suggest that mutations in this region will be important for function. In 1998 Traynelis et al. (*34*) showed that the same mutation also leads to a decrease in Zn^{2+} voltage inhibition of NR1/NR2A receptors. Both of these reports indicate that removal of this disulfide bridge converts the receptor into a state that can be opened more readily. In addition, comparison of the crystal structures of NR1 LBD with DCKA (1PBQ) and glycine (1PB7) shows that domain closure results in a movement of the end of helix K (adjacent to the C744−C798 bond) toward the binding cleft. Furukawa and Gouaux (*16*) suggested that removal of this disulfide bond releases a constraint on this rearrangement, which facilitates domain closure and agonist binding.

Two further disulfide bridges are observed in the crystal structures, both of which occur in loop 1: C420−C454 and C436−C455. Loop 1 has been postulated to form part of the subunit interface in the tetrameric assembly (*16*), and thus stability in this region may be crucial in receptor modulation. The effects of these disulfide bridges, and indeed whether they are always present, have been the subject of several experiments. Mutation of residues C420 or C436 to alanine, which presumably destroys either disulfide bridge, was shown to lead to an ∼15-fold reduction in relative potentiation by glycine and glutamate for NR1/NR2B receptors (*35*). However, it is not clear in those experiments what the receptor composition is. It has been shown in *Xenopus* oocytes that removal of glycine leads to a reduced NMDA response (*36*), but it is only partial and thus at odds with the proposal that glycine is a true coagonist (*37*). There are a number of suggestions for this observation including (i) the proposal that the NR1 subunit can form a homomeric receptor and (ii) that the NR1 subunit can form a heteromeric receptor with other endogenous *Xenopus laevis* subunits [though not apparently the XenU1 subunit (*38*)]. These factors become relevant to the experiments reported by Laube et al. (*35*) because the current formed by these "homomeric" receptors is small (less than 40 nA), which is the same order of magnitude of current reported for several mutations (including those of C420 and C436). The issue is further compounded by the fact that glycine contamination is a problem with NMDA receptor studies (*3*, *39*, *40*); indeed, responses to concentrations as low as 10 nM have been reported (*3*). Thus, structural interpretation of the work of Laube et al. (*35*) is not straightforward.

Interestingly, Köhr et al. (*41*) found that, for the same mutations (C420 and C436), reducing agents (dithiothreitol or glutathione) could potentiate whole cell currents as was the case for wild-type receptors. Thus it appears that the allostery between subunits may be separable from the potentiating effects of reducing agents. These effects may stem from different conformations at the interface between subunits or differences in the dynamics of the subunits or a combination of both. Interestingly, both groups (*35*, *41*) found that mutating residues C454 and C455 to alanine had

Table 1: Summary of Simulations

simulation	duration (ns)	description
open-apo	20	ligand removed from 1PBQ (antagonist-bound structure)
C744A-C798A	20	as open-apo but with C744 and C798 mutated to alanine to destroy the SS bond
C744A-C798A-Gly	20	as glycine bound (1PB7) but with C744 and C798 mutated to alanine to destroy the SS bond
C454*	20, 10	as open-apo with no mutations but no SS bond between C454 and C420[a]
C454A-C455A	20	as open-apo but with C454 and C455 mutated to alanine to destroy the two SS bonds (between C454−C420 and C455−C436)[b]
C420A-C436A	20, 10	as open-apo but with C420 and C436 mutated to alanine to destroy the two SS bonds (between C454−C420 and C455−C436)[a]

[a] Two 10 ns runs were also performed but with different initial velocities. [b] A new disulfide bond was created between C420 and C436. See the Methods section of the main text for details.

no effect on the receptor. Köhr et al. (*41*) did find, however, that mutating these residues in the NR2A subunit engendered a loss of channel activity, which has led to the proposition that adjacent cysteines found at homologous positions of NR1 and NR2 subunits are not functionally equivalent. Additionally, Furukawa and Gouax (*16*) report that there is alternate electron density for C454 which would preclude the formation of a disulfide bond with C420.

Considering these data and the overall view that NMDA receptors are modulated by redox agents (*42*), we were interested to see to what extent the presence or absence of combinations of these disulfide bridges had on the underlying dynamics of the ligand-binding domain. We consider the C744A-C798A double mutation (both open cleft and closed cleft, with glycine bound), the possibility of the alternative density at C454, and another double mutation of C420A-C436A. We also examined the double mutation C454A-C455A but hypothesized that mutations in these residues could be compensated for by a new disulfide bridge formed between C420 and C436 which we included in the simulation (Figure 1C−F and Table 1). We have used atomistic molecular dynamics to investigate the effects of these mutations. MD and other theoretical methods have recently been applied to the ligand-binding domains of both AMPA (*43*−*50*), kainate (*51*, *52*), and NMDA receptors (*53*, *54*) and provide a complementary approach to the physiological, pharmacological, and structural methods. For a review see ref *55*.

Our molecular dynamics (MD) simulations demonstrate (i) a potential mechanism by which the C744A-C798A mutation may confer potentiation, (ii) that removing two disulfide bonds in loop 1 (C420 and C436) results in a ligand-binding domain that has a tendency to close but not induce the change in hinge conformation associated with the presence of full agonist, and (iii) C454 when not oxidized appears to exist in two different states defined by $\chi 1$ (side-chain rotation about the Cα−Cβ bond), which is in agreement with the observation of alternate electron density observed.

METHODS

System Preparation. Coordinates for the crystal structure of the NR1 with 5,7-dichlorokynurenic acid (DCKA) bound (1PBQ) and glycine bound (1PB7) were downloaded from www.rcsb.org. An open-apo state was generated from 1PBQ by removing the ligand and used as the basis for all mutants generated, except the glycine bound where 1PB7 was used. We chose an open-cleft form of the protein as we expected it to have the greatest flexibility (*54*) and therefore reveal any effects due to mutations in the shortest time window. We generated a total of six simulation systems by both mutating key cysteine residues to alanines and in one case removing a disulfide bond from the system setup. Two simulations were repeated with different initial velocities, thus providing 140 ns of simulation time. Table 1 summarizes the simulations which were designed to explore the changes in dynamics that may result from a change in the disulfide bonds.

The N and C termini were acetylated and amidated, respectively, to mimic the continuation of the peptide chain. Missing side chains were built in using the WHATIF "complete a structure" web service (http://swift.cmbi.kun.nl/WIWWWI/). As the initial structure did not have part of loop 1 (away from the cysteine residues of interest) resolved in the crystal structure, we used Modeller v7 (*56*) to generate the missing residues as described previously (*54*). A comparison between our generated loop and the crystallographically resolved loop from a closed-cleft structure [1-aminoyclopropanecarboxylic acid (ACPC), 1Y20] is detailed in Supporting Information (supplementary Figure 1).

Simulation Parameters. The resulting structures were then solvated in a cubic box with ~25000 simple point change (SPC) waters (*57*) and counterions added to ensure overall electrostatic neutrality. All simulations were performed with Gromacs 3.1.4 (*58*, *59*), with the ffgmx force field and the NPT ensemble at 300 K using the Berendsen thermostat (*60*). The influence of the force field was tested by performing a repeat simulation of the open-apo system with the 53a6 force field (*61*), and no significant changes were found on these time scales. The pressure was coupled with the Berendsen barostat with a coupling constant, τ, of 1.0 ps. Electrostatics were calculated using the Particle Mesh Ewald method (*62*, *63*) with a short-range cutoff of 10 Å. The time step for integration was 2 fs. The LINCS algorithm (*64*) was used to restrain bond lengths. Each system was subjected to a 200 ps dynamics run with the protein restrained (10 kJ mol^{-1} Å^{-2} on all heavy atoms). This was followed by 20 ns of free simulation. The only variation in this setup was that the C454A-C455A simulation was subjected to a 1 ns run after the positional restraints were removed. During this time distance restraints were placed on the sulfur atoms of C420 and C436 (using a force constant of 1000 kJ mol^{-1} Å^{-2}) to pull them to a distance of ~3 Å. A disulfide bond was then created between the two residues, the distance restraints were removed, and the simulation was allowed to continue in the same manner as the others.

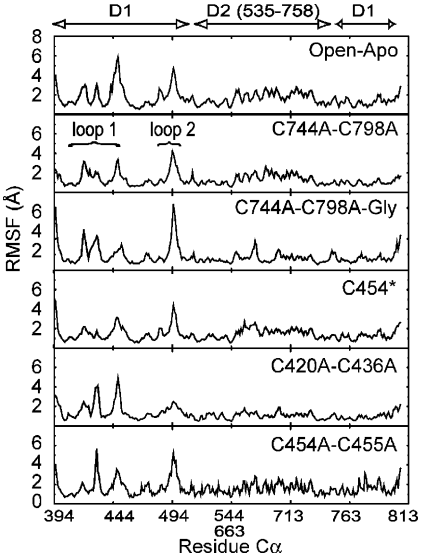

FIGURE 2: Root mean square fluctuations (RMSF) for the simulations calculated from 2 to 20 ns. Data from only one simulation for the C454* and the C420A-C436A simulations are shown for clarity. The results from the second simulations are similar. The large peaks correspond to the positions of loops 1 and 2, which are conformationally flexible.

Hydrogen bonds were calculated using the g_hbond program from Gromacs with a 30° angle and a 3.5 Å radius. All calculations were performed on a Linux cluster. In the case of the C454A-C455A simulation, analysis is compared back to the structure at the end of the pulling phase rather than the crystal structure.

RESULTS

Protein Motion. Figure 2 shows the root mean square fluctuation (RMSF) of each Cα atom. This is a measure of residue flexibility with peaks representing more mobile regions of the protein. In nearly all of the simulations there are peaks that correspond to the location of the loops in D1; 415−419, 425−428, and 439−451 are in loop 1 and residues 486−497 are located in loop 2. In general, it can be said that residues have the highest fluctuation for the C454A-C455A mutation and the lowest fluctuation for the C420A-C436A mutation. These results confirm that the mutations do not drastically alter the general behavior of the protein compared to the wild type (open-apo) on these time scales. Results for both sets of simulations with different initial velocities for the C454* and C420A-C436A simulations were similar, and thus only analysis from one trajectory in each case is presented for clarity unless otherwise stated.

In order to examine the motion further, we analyzed the root mean square deviations (RMSD) of the individual domains, D1 and D2. The RMSD of Cα atoms relative to an initial structure is a standard measure of structural drift over time. Figure 3A shows the Cα RMSD of the D1 domains fitted onto the D1 domain. All except the C744A-C798A simulation plateau off at levels between 3 and 5 Å. The C744A-C798A simulation plateaus off at ∼2.5 Å. Closer inspection of this trajectory revealed that residues from loop 1 were able to make strong interactions with residues located in helix K thus stabilizing D1 (discussed below). We speculated that the large drift for D1 Cα atoms might be predominantly attributable to the two large loops (loop 1 and loop 2) in the D1 domain and so performed an RMSD calculation on the D1 Cα but this time omitting Cα that form these loops. The results are shown in Figure 3B and demonstrate that this indeed appears to be the case with all of the plateaus being less than 3 Å and generally closer to 2 Å.

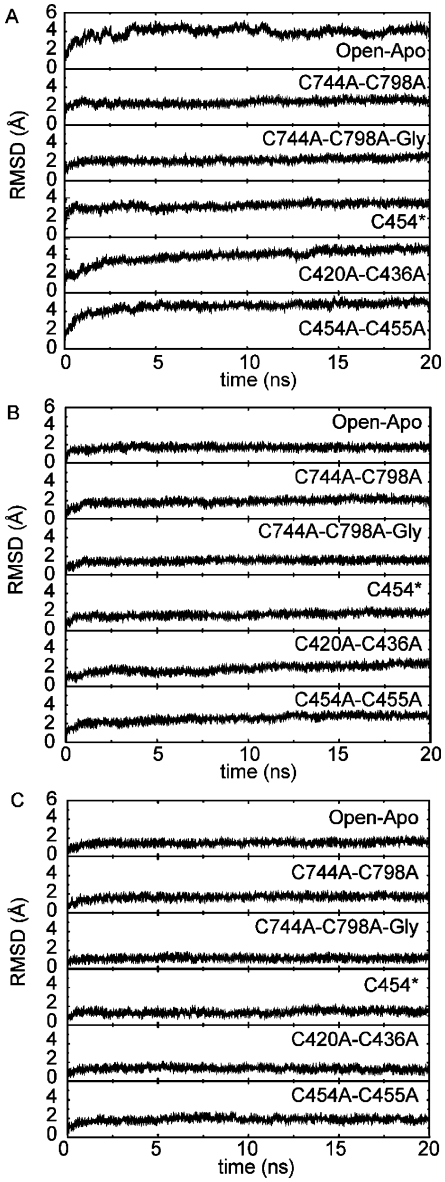

FIGURE 3: RMSD plots for the simulations (one simulation from the C454* and C420A-C436A trajectories for clarity; results are similar from the second runs) of (A) D1 Cα fitted onto D1 Cα, (B) D1 Cα fitted onto D1 Cα excluding loops 1 and 2, and (C) Cα from D2 fitted onto the Cα of D2.

We also calculated the RMSD of the Cα atoms of D2 (with respect to D2). Figure 3C shows that the drift in this domain is lower than D1 and is more consistent with all of the simulations converging to ∼1.75 Å. From Figure 3A we note that the highest drift generally appears in the two simulations with loop 1 mutations (C420A-C436A and C454A-C455A). This could be attributable to the fact that these simulations have removed two of the original disulfide bonds, thus creating a more flexible structure.

We examined the behavior of loop 1 in all simulations. There are number of common interactions (listed in Table 2) that predominate in all simulations. Most of these are

Table 2: Summary of Conserved Interactions between Loop 1 and the Rest of the Protein

residue	residue	residue	residue
T414	P452	T437	H477
K432	D461	T437	L478
V434	C455	G438	V451
C436	Q453	T442	A480
T437	V476	T442	D481

backbone−backbone interactions reflecting the sheet structure of the loop. Backbone−backbone interactions were not affected in the simulations where a cysteine had been mutated to alanine. We did note one interesting side-chain−side-chain interaction between K432 in loop 1 and D461 on helix B. This aspartic acid at position 461 is conserved in glutamate receptors. Position 432 is either a lysine or proline in NR1 subunits, arginine or glutamine in NR2 subunits, and leucine in NR3 subunits. This residue is part of the extended loop 1 that is not present in non-NMDA receptors. It may be that this serves as an anchor for loop 1 in most NR1 and NR2 subunits.

Throughout the simulations, loop 1 interacts with helix K (and residues C-terminal to this helix). The exact nature and number of contacts differ in the simulations, but there are a couple of general observations that can be made. The residues involved are typically V426, N427, and D429 from loop 1 and residues T791, R794, Q796, and E797 from helix K onward. The polar nature of most of these residues combined with exposure of backbone groups of residues subsequent to helix K means that there is a mixture of side-chain to backbone hydrogen bonds from both regions of the protein. Once the hydrogen bonds were established, loop 1 tended to remain in that position for the duration of the simulation. The only simulation where this was not observed was the C454A-C455A. In this simulation, loop 1 was held in approximately the same conformational space as the other simulations, but by the forming of a hydrogen bond between the side-chain carboxylic acid group of D429 and the OH group of Y795. Another interaction that was observed in all but the C794A-C798A-Gly and C454A-C455A simulations was the D429 side-chain carboxylic acid group interacting with the OH group of T791.

In the C744A-C798A mutants, the exposure of polar backbone groups from helix K through to the C terminus (which enables them to form hydrogen bonds with residues in loop 1) is facilitated by the absence of the disulfide bond. Indeed, there is an increase in the fraction of coil structure in this region, as defined by DSSP (*65*) in these simulations compared to the simulations where this disulfide is maintained. This allows backbone−backbone interactions to form as shown in Figure 4A,B. Q796 and E797 form hydrogen bonds to the backbone carbonyl groups of V426 and N427 (in loop 1). The displacement required to form these interactions is not large. The difference in the distance between the Cα of residues in 744 and 798 for the mutant and wild type is shown in Figure 4C and shows an approximate movement of 3 Å.

The intersubdomain distance is used to measure changes in the extent of domain closure as a function of time. The distance is defined as the distance between the center of mass between the D1 and D2 subdomains. Figure 5A shows this distance as a function of time for the simulations. The open-

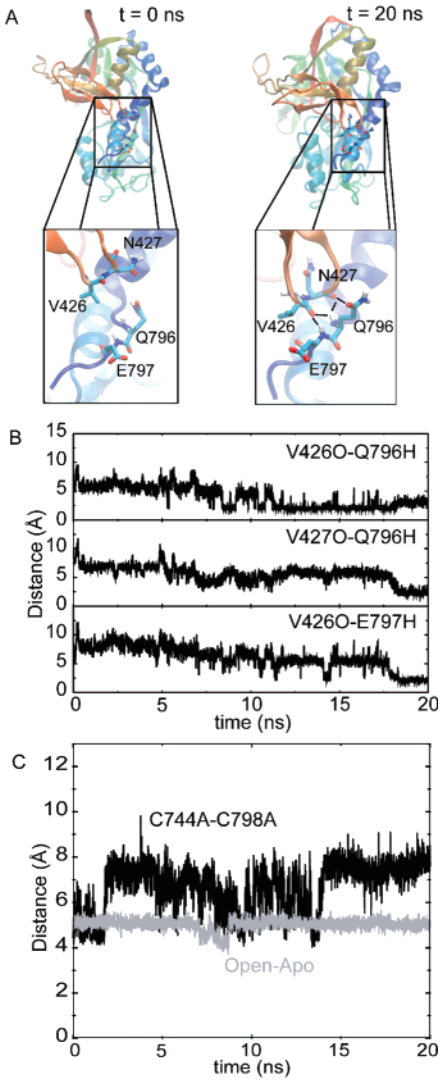

FIGURE 4: (A) shows the region responsible in the C744A-C798A simulation that stabilized the D1 domain. There are interactions between the backbone groups of helix K and loop 1. (B) shows the evolution of these interactions (which are not present in the starting configuration based on open-apo), and (C) shows the distance between Cα atoms of these residues in the C744A-C798A simulation (black) compared to open-apo (gray line).

apo, C454*, and C454A-C455A simulations all maintain separations consistent with an open-cleft form of the protein, while the C744A-C798A-Gly simulation clearly stays closed (actually a little more closed than the crystal structure) as would be expected for a subunit with ligand bound. In the case of the open-apo and the C454* simulations there are significant periods of "hyperextension", between 5 and 7 ns and 6 and 11 ns, respectively. Recent crystal structures of GluR5 in complex with antagonists suggested that the ligand-binding domain of glutamate receptors may be able to open more than previously first thought on the basis of earlier crystal structures (*66*). By contrast, recent fluorescence resonance energy transfer (FRET) studies on the GluR2 ligand-binding domain suggest that changes in the extent of cleft closure between apo and agonist-bound states is smaller than that observed in the crystal structures (*67*). Clearly, this issue is complicated and not yet fully understood. C420A-C436A undergoes an initial closing of the domains to a level seen in the glycine-bound crystal structure (represented by

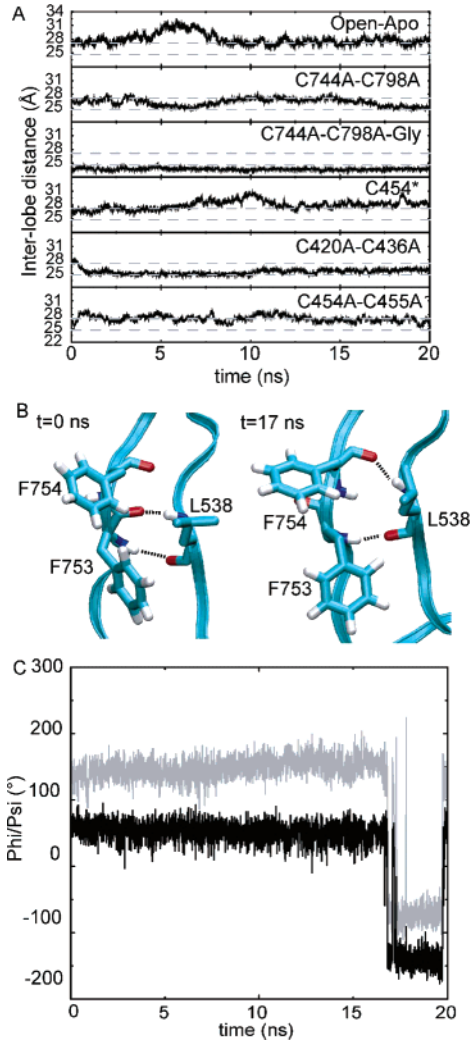

FIGURE 5: (A) shows the interlobe separation for each of the simulations calculated by taking the distance between the center of mass for each subdomain (D1 or D2). The dashed gray lines indicate the extremes that have been observed by X-ray crystallography (24.7 Å for the closed state from 1PB7 and 27.2 Å for an antagonist-bound state from 1PBQ). It can be seen that removal of the disulfide bond between C744 and C798 allows the two lobes to move between the open and closed states more readily than in the other proteins. Data from only one trajectory for the C454* and C420A-C436A were used for clarity. Results are similar in both cases. (B) Snapshots of the C774A-C798A simulation showing the reorientation of the hinge residues that has been proposed to be indicative of a full-agonist binding. (C) Change in hinge residue backbone torsion angles with time; 753 ϕ (black) and 754 ψ (gray). Although there is a cleft closure at 5 ns, as indicated in (A), there is no corresponding change in the hinge torsions. However, during the second cleft closure event at 17 ns, a change in the hinge residue torsion angles is observed.

the lower dashed gray line in Figure 5A) and remains approximately there for the rest of the 20 ns simulation.

The C744A-C798A simulation is more flexible, opening and closing slightly several times as would be expected from the hypothesis put forward by Furukawa and Gouaux (*16*) which postulated that removal of this disulfide would allow greater flexibility of this region which would facilitate domain movement. Over 20 ns of simulation the C744A-C798A simulation closes to a degree consistent with an agonist-bound LBD more than once, with degrees of closure similar to the glycine-bound crystal structure occurring between 5 and 7 ns and again between 17 and 20 ns. Movement of iGluR LBDs between closed-cleft and open-cleft conformations in the absence of agonist is not without precedent; small-angle X-ray scattering (SAXS) experiments on GluR2 indicated that the time-averaged conformation of the ligand-free LBD in solution is intermediate between the open, antagonist-bound state and the closed, agonist-bound state, suggesting a conformational equilibrium (*68*). Furthermore, a closed-cleft apo form of the bacterial glutamate receptor, GluR0, has been observed crystallographically (*69*). We have previously reported domain closure in the absence of ligand for the GluR2 subunit (*50*) and the NR1 subunit (*54*) in simulation studies.

The apparent tendency of the protein from the C744A-C798A simulation to move more readily between open and closed forms prompted us to examine the hinge region of the LBD. It has been suggested that the conformation of the hinge region between D1 and D2 can be an indicator of a full agonist bound and thus an indicator of channel potentiation (*16*, *54*). We found that during the first period of closure between 5 and 7 ns the hinge was in a conformation that was indicative of an antagonist being present (Figure 5B,C). However, in the second period of closure we found that the ψ of F753 and the ϕ of F754 rotated into conformations more consistent with an agonist-bound conformation. Interestingly in the C744A-C798A-Gly simulation, we found that the hinge can flip into a conformation consistent with an antagonist-bound conformation. As we do not see any change in hinge conformation in any of the other six simulations, this suggests that removal of this disulfide bond appears to influence the dynamics of the hinge region. Although we observe that the C420A-C436A simulation adopts a more closed-cleft structure during this period, there was no change in the conformation in the hinge region.

C454 Simulation.* The C454* simulation in which no mutations were made, but the disulfide bond to C420 is absent, was performed to test the effect of omitting one disulfide bond. Furthermore, it was reported that there was alternative electron density for this residue in the recent crystallographic study (*16*). The omission of this disulfide bond means that there is only the C455−C436 disulfide bond in loop 1. It appears from the RMSD analysis (Figure 3) and the interlobe separation (Figure 5A) that this simulation behaves similarly to the wild-type open-apo simulation. The RMSF data (Figure 2), however, indicate that there is less fluctuation in loop 1 compared to the other simulations. Closer examination of the C454* simulation revealed that this residue can spend a considerable amount of time with the side chain in an alternate position, which would preclude the formation of the disulfide bond with C420. Figure 6A shows a histogram analysis of the χ1 torsion (N−Cα−Cβ−Sγ). There are two main peaks centered around 60° and −60°. There is a very small peak at −165° which corresponds to the orientation of χ1 found in the open-apo (and other) simulations. The time course of distance between the sulfur atoms of residues C420 and C454 is shown in Figure 6B. Consistent with the histogram data, there appear to be two major conformational states, one of which places these atoms less than 3.5 Å from each other, which would presumably be close enough to allow a disulfide bond to form if conditions allow. We suggest that if a disulfide bond is formed, it pulls the χ1 torsion to −165°. Our results show little difference in the behavior of the LBD whether this

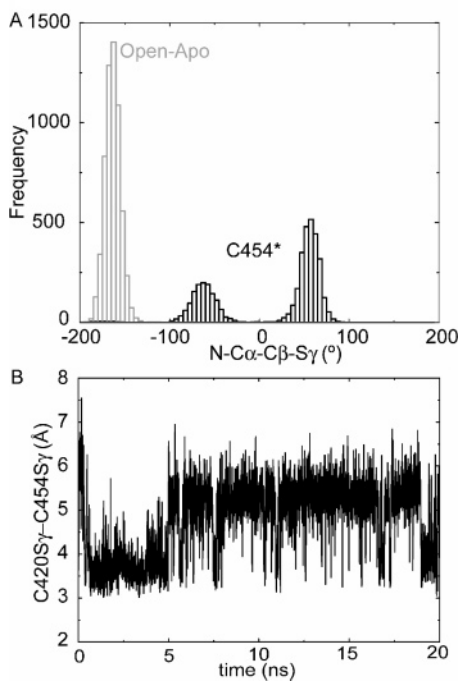

FIGURE 6: (A) shows the distribution of the N−Cα−Cβ−Sγ torsion (χ1) for the open-apo (gray) and the C454* simulation (black). Although there are two major populations for the C454*, there is also a very small population located at the same position as the open-apo. (B) shows the variation of the distance between the sulfur atoms of C420 and C454 with time.

disulfide bond is present or not, in agreement with the experimental observations of Köhr et al. (*41*), who reported that mutating just one of the loop 1 cysteines had no effect on the potentiation (by reducing agents) of the NMDA receptor.

DISCUSSION

The NMDA receptor has a wide variety of ways in which it can "tune" its response to environmental conditions. One of these is the influence of redox conditions on the formation of disulfide bridges, and indeed this has been investigated by site-directed mutagenesis by several groups (*20*, *35*, *41*, *42*). The redox modulation of proteins may be a quite general mechanism of regulation (*70*). In this work we have used molecular dynamics to try to address the role of the disulfide bridges that can occur within the ligand-binding domain of NR1. It should be remembered that the overall time scale of gating in the full-length receptor is of the order of milliseconds and our time scale here is 20 ns. However, it has been demonstrated that relevant motions for these receptors can be discerned on these time scales (*50*, *54*). The simulations thus provide insight into the way in which the formation of disulfide bridges controls the behavior of the receptor. Our simulations behave in a manner similar to those observed in wild type and to those observed previously for this receptor (*54*), to GluR2 (*50*), and to the related periplasmic binding proteins (*71*). Thus the mutations do not affect the overall behavior of the protein dynamics. The behavior of the two lobes is quite distinct and directly reflects the positions of the cysteines in D1. The D2 behavior is similar in all of the simulations on this time scale and suggests that D2 may simply behave as a rigid body through which the modulatory effects are transmitted. NMR experiments on the GluR2 ligand-binding domain, however, indicate that there are conformational dynamics in D2 on a microsecond to millisecond time scale that show agonist dependencies (*72*) and that also might allow ligand dissociation without the need for cleft opening (*73*).

Experiments whereby the disulfide between C744 and C798 is removed are consistent in their interpretation with Sullivan and colleagues (*33*) reporting a 6-fold decrease in the EC_{50} and Traynelis and colleagues (*34*) reporting a decrease in the voltage-independent Zn^{2+} inhibition of NR1/NR2A receptors. It has been proposed that removal of this disulfide allows helix K to move more readily and facilitates domain closure and agonist binding (*16*). Our analysis of the interlobe movement appears to support this proposal, even on this time scale. This suggests that the relative motions of two semirigid bodies (D1 and D2) can be influenced by one flexible tether (the disulfide bond). Our results suggest that the lack of a disulfide bond in this region allows this subunit greater flexibility which consequently will affect the allosteric interaction with the NR2 subunits. These allosteric interactions presumably manifest themselves with a change in the EC_{50} value for agonists that act both at NR1 and at NR2. The EC_{50} value, although a useful value, encompasses a wide range of mechanisms and effects into one number (*74*). Our results suggest that there may indeed be other important effects that need to be considered including, for example, the influence of these dynamics on the conformation of the hinge region. It has been suggested (*16*, *54*) that the conformation of the hinge region can be an indicator of whether a full agonist is bound or not and hence indirectly reflects the state of the receptor. Our simulations suggest that in the C744A-C798A mutants helix K may be allowed to unwind enough to more readily promote interactions with part of loop 1 and with hinge residue K534. We therefore suggest that the C744A-C798A mutant not only exhibits greater interdomain flexibility but can also induce increased flexibility to the hinge region and, thus, can play a role in determining the EC_{50} for agonists that act at the NR2 subunit via allosteric interactions.

The crystal structure suggested that there are two additional disulfide bonds: C420−C454 and C436−C455. Their role in the behavior of the receptor is, however, still unclear. Our observation that the C420A-C436A simulation adopted a more closed cleft might lead one to conclude that access to the binding site is somehow hindered in this mutant. However, Laube et al. (*35*) found that mutant EC_{50}s were similar to wild-type receptors, implying that low current responses were not caused by a reduction in binding affinities. The experiments of Köhr et al. showed that potentiation by reducing agents is similar in these mutants to wild-type receptors (*41*). Both groups, however, reported that mutation of C454 or C455 resulted in very little effect. Thus, these data do not provide a straightforward picture of how redox conditions might control the protein. Even where there is agreement from both Laube and Köhr (i.e., that mutation of both C454 or C455 results in little difference in the behavior of the receptor), it is not readily explained by the crystal structure, which suggests that this would destroy at least one disulfide bridge. There are a number of ways in which the redox-related changes in receptor behavior might be explained. For example, it might be that the subunit

interface is changed by these mutations and thus changes the allosteric coupling between subunits.

Support for this comes from experiments which showed that loop 1 of NR2A allosterically couples the binding of glutamate on an NR2A subunit to the binding of glycine on an NR1 subunit (*75*). Furthermore, on the basis of the crystal structure and a comparison with GluR2 crystal structures, it was proposed that some residues in loop 1, including V426, might interact with residues of an adjacent subunit (*16*). Another explanation might be that the underlying dynamics of the LBD are altered in the mutants which also affects the manner in which the subunits are coupled. Our simulations were designed in such a way as to explore this latter point. We considered three possibilities that we thought would manifest changes in as short a time as possible: (i) removal of one disulfide bridge, (ii) removal of both disulfide bridges, and (iii) the possibility of an alternative disulfide bridge. We reasoned that mutating C454 or C455 might not result in a drastic change in function if a different disulfide bridge was allowed to form between C420 and C436.

In the case where neither of the crystallographically located disulfide bridges were present (C420A-C436A), we found that the domain closed up with respect to wild type but was never in a fully closed conformation. Loop 1 is large (38 residues), and we suggest from this that removal of these disulfides could render this segment more flexible, and thus this could result in conformations that hinder agonist binding either by inducing a more closed state or by physical occlusion of the binding pocket. As our results from C454* (where only one disulfide bridge is broken) are similar to the "wild type" (open-apo), we suggest that both disulfide bridges would have to removed to observe a change in the behavior of the receptor. Interestingly, where we introduced an alternative disulfide arrangement, the behavior of the protein is very similar to that of the wild type (open-apo).

We believe these simulations help to rationalize some of the conflicting data, but we should also note two limitations to this work. The first is that these simulations only consider the monomeric form of the ligand-binding domain. Currently, we do not fully understand the relationship of the dynamics between each subunit in the full-length receptor. Furthermore, we are not able to examine cross-subunit disulfide bridges. Although we have focused here on the intrasubunit dynamic contribution, it is likely that this forms part of the broader intersubunit interaction that is likely to underpin the coupling between subunits. In the case of NMDA receptors, a lack of detectable concentration dependence suggested that channel opening cannot occur with less than all four binding sites occupied (*30*), thus demonstrating that the coupling between the ligand-binding domains is essential. Another limitation is the time scale of these simulations; more subtle or equilibrium-based observations would require much longer simulation times than those which have been performed here. Despite these limitations, the simulations do provide insight into the manner in which these proteins may be regulated by redox conditions.

CONCLUSIONS

The redox properties of NMDA receptors are complex and intricate. Some of the experiments concerning the effects of the cysteine residues in the protein are difficult to reconcile with each other in light of the current structural data. Our simulations, while not able to fully resolve all of the differences, have allowed us to offer some explanations for these effects. We have provided a plausible explanation as to why C454 or C455 can be mutated to alanine with apparently no effect on the behavior of the receptor. However, the clearest result appears to be the C744A-C798A mutation for which we are able to observe an increase in interdomain flexibility and an apparent increase in the flexibility of the hinge region. Both of these observations suggest that the lower NMDA EC_{50} observed experimentally is a result of allosteric interactions. An NR1 subunit that undergoes ligand-binding domain transitions more readily will also promote NR2 ligand-binding domain transitions. An understanding of these allosteric mechanisms and how they are influenced by endogenous ligands in vivo is essential if we are to identify function-specific ligands (*76*).

ACKNOWLEDGMENT

We thank the Oxford Supercomputing Centre.

SUPPORTING INFORMATION AVAILABLE

One figure as described in the text. This material is available free of charge via the Internet at http://pubs.acs.org.

REFERENCES

1. Dingledine, R., Borges, K., Bowie, D., and Traynelis, S. F. (1999) The glutamate receptor ion channels, *Pharmacol. Rev. 51*, 7−61.
2. Cull-Candy, S., Brickley, S., and Farrant, M. (2001) NMDA receptor subunits: diversity, development and disease, *Curr. Opin. Neurobiol. 11*, 327−355.
3. Johnson, J. W., and Ascher, P. (1987) Glycine potentiates the NMDA response in cultured mouse brain neurons, *Nature 325*, 529−531.
4. Mothet, J.-P., Parent, A. T., Wolosker, H., Brady, R. O., Linden, D. J., Ferris, C. D., Rogawski, M. A., and Snyder, S. H. (2000) D-Serine is an endogenous ligand for the glycine site of the *N*-methyl-D-aspartate receptor, *Proc. Natl. Acad. Sci. U.S.A. 97*, 4926−4931.
5. Shleper, M., Kartvelishvily, E., and Wolosker, H. (2005) D-serine is the dominant endogenous coagonist for NMDA receptor neurotoxicity in organotypic hippocampal slices, *J. Neurosci. 25*, 9413−9417.
6. Kartvelishvily, E., Shleper, M., Balan, L., Dumin, E., and Wolosker, H. (2006) Neuron-derived D-serine provides a novel means to activate *N*-methyl-D-aspartate receptors, *J. Biol. Chem. 281*, 14151−14162.
7. Schorge, S., and Colquhoun, D. (2003) Studies of NMDA receptor function and stoichiometry with truncated and tandem subunits, *J. Neurosci. 23*, 1151−1158.
8. Banke, T. G., and Traynelis, S. F. (2003) Activation of NR1/NR2B NMDA receptors, *Nat. Neurosci. 6*, 144−152.
9. Chatterton, J. E., Awobuluyi, M., Premkumar, L. S., Takahashi, H., Talantova, M., Shin, Y., Cui, J., Tu, S., Sevarino, K. A., Nakanishi, N., Tong, G., Lipton, S. A., and Zhang, D. (2002) Excitatory glycine receptors containing the NR3 family of NMDA receptor subunits, *Nature 415*, 793−798.
10. Sommer, B., Kohler, M., Sprengel, R., and Seeburg, P. H. (1991) RNA editing in brain controls a determinant of ion flow in glutamate-gated channels, *Cell 67*, 11−19.
11. Robbins, T. W., and Murphy, E. R. (2006) Behavioural pharmacology: 40+ years of progress, with a focus on glutamate receptors and cognition, *Trends Pharmacol. Sci. 27*, 141−148.
12. Dirnagl, U., Iadecola, C., and Moskowitz, M. A. (1999) Pathobiology of ischemic stroke: An integrated view, *Trends Neurosci. 22*, 391−397.
13. Obrenovitch, T. P., and Urenjak, J. (1997) Is high extracellular glutamate the key to excitotoxicity in traumatic brain injury, *J. Neurotrauma 14*, 677−698.

14. Chazot, P. L., and Hawkins, L. M. (1999) NMDA receptor subtypes—rationale for future CNS therapies, *IDrugs 2*, 1313−1326.
15. Sack, J. S., Saper, M. A., and Quiocho, F. A. (1989) Periplasmic binding protein structure and function. Refined X-ray structures of the leucine/isoleucine/valine-binding protein and its complex with leucine, *J. Mol. Biol. 206*, 171−191.
16. Furukawa, H., and Gouaux, E. (2003) Mechanisms of activation, inhibition and specificity: crystal structures of the NMDA receptor NR1 ligand-binding core, *EMBO J. 22*, 2873−2885.
17. Inanobe, A., Furukawa, H., and Gouaux, E. (2005) Mechanism of partial agonist action at the NR1 subunit of NMDA receptors, *Neuron 47*, 71−84.
18. Jang, M.-K., Mierke, D. F., Russek, S. J., and Farb, D. H. (2004) A steroid modulatory domain on NR2B controls N-methyl-D-aspartate receptor proton sensitivity, *Proc. Natl. Acad. Sci. U.S.A. 101*, 8198−8203.
19. Rachline, J., Perin-Dureau, F., Le Goff, A., Neyton, J., and Paoletti, P. (2005) The micromolar zinc-binding domain on the NMDA receptor subunit NR2B, *J. Neurosci. 25*, 308−317.
20. Lipton, S. A., Choi, Y.-B., Takahashi, H., Zhang, D., Li, W., Godzik, A., and Bankston, L. A. (2002) Cysteine regulation of protein function—as exemplified by NMDA-receptor modulation, *Trends Neurosci. 25*, 474−480.
21. Papadakis, M., Hawkins, L. M., and Stephenson, F. A. (2004) Appropriate NR1-NR1 disulphide-linked homodimer formation is requisite for efficient expression of functional, cell surface *N*-methyl-D-aspartate NR1/NR2 receptors, *J. Biol. Chem. 279*, 14703−14712.
22. Furukawa, H., Singh, S. K., Mancusso, R., and Gouaux, E. (2005) Subunit arrangement and function in NMDA receptors, *Nature 438*, 185−192.
23. Armstrong, N., Sun, Y., Chen, G.-Q., and Gouaux, E. (1998) Structure of a glutamate-receptor ligand-binding core in complex with kainate, *Nature 395*, 913−917.
24. Armstrong, N., and Gouaux, E. (2000) Mechanisms for activation and antagonism of an AMPA-sensitive glutamate receptor: Crystal structures of the GluR2 ligand binding core, *Neuron 28*, 165−181.
25. Hogner, A., Kastrup, J. S., Jin, R., Liljefors, T., Mayer, M. L., Egebjerg, J., Larsen, I. K., and Gouaux, E. (2002) Structural basis for AMPA receptor activation and ligand selectivity: crystal structures of five agonist complexes with the glur2 ligand-binding core, *J. Mol. Biol. 322*, 93−109.
26. Naur, P., Vestergaard, B., Skov, L. K., Egebjerg, J., Gajhede, M., and Kastrup, J. S. (2005) Crystal structure of the kainate receptor GluR5 ligand-binding core in complex with (*S*)-glutamate, *FEBS Lett. 579*, 1154−1160.
27. Mayer, M. L. (2005) Crystal structures of the GluR5 and GluR6 ligand binding cores: molecular mechanisms undelying kainate receptor selectivity, *Neuron 45*, 539−552.
28. Nanao, M. H., Green, T., Stern-Bach, Y., Heinemann, S. F., and Choe, S. (2005) Structure of the kainate receptor subunit GluR6 agonist-binding domain complexed with domoic acid, *Proc. Natl. Acad. Sci. U.S.A. 102*, 1708−1713.
29. Mayer, M. L. (2006) Glutamate receptors at atomic resolution, *Nature 440*, 456−462.
30. Schorge, S., Elenes, S., and Colquhoun, D. (2005) Maximum likelihood fitting of single channel NMDA activity with a mechanism composed of independent dimers of subunits, *J. Physiol. 569*, 395−418.
31. Auerbach, A., and Zhou, Y. (2005) Gating reaction mechanisms for NMDA receptor channels, *J. Neurosci. 25*, 7914−7923.
32. Kristensen, A. S., Geballe, M. T., Snyder, J. P., and Traynelis, S. F. (2006) Glutamate receptors: Variation in structure-function coupling, *Trends Pharmacol. Sci. 27*, 65−69.
33. Sullivan, J. M., Traynelis, S. F., Chen, H. S., Escobar, W., Heinemann, S. F., and Lipton, S. A. (1994) Identification of two cysteine residues that are required for redox modulation of the NMDA subtype of glutamate receptor, *Neuron 13*, 929−936.
34. Traynelis, S. F., Burgess, M. F., Zheng, F., Lyuboslavsky, P., and Powers, J. L. (1998) Control of voltage-independent zinc inhibition of NMDA receptors by the NR1 subunit, *J. Neurosci. 18*, 6163−6175.
35. Laube, B., Kuryatov, A., Kuhse, J., and Betz, H. (1993) Glycine-glutamate interactions at the NMDA-receptor: role of cysteine residues, *FEBS Lett. 335*, 331−334.
36. Moriyoshi, K., Masu, M., Ishii, T., Shigemoto, R., Mizuno, N., and Nakanishi, S. (1991) Molecular cloning and characterization of the rat NMDA receptor, *Nature 354*, 31−37.
37. Kleckner, N. W., and Dingledine, R. (1988) Requirement for glycine in activation of NMDA-receptors expressed in *Xenopus* oocytes, *Science 241*, 835−837.
38. Green, T., Rogers, C. A., Contractor, A., and Heinemann, S. F. (2002) NMDA receptors formed by NR1 in *Xenopus laevis* oocytes do not contain the endogenous subunit XenU1, *Mol. Pharmacol. 61*, 326−333.
39. Pittaluga, A., and Raiteri, M. (1990) Release-enhancing glycine-dependent presynaptic NMDA receptors exist on noradrenergic terminals of hippocampus, *Eur. J. Pharmacol. 191*, 231−234.
40. Paudice, P., Gemignani, A., and Raiteri, M. (1998) Evidence for functional native NMDA receptors activated by glycine or D-serine alone in the absence of glutamatergic coagonist, *Eur. J. Neurosci. 10*, 2934−2944.
41. Köhr, G., Eckardt, S., Lüddens, H., Monyer, H., and Seeburg, P. H. (1994) NMDA receptor channels: Subunit-specific potentiation by reducing agents, *Neuron 12*, 1031−1040.
42. Aizenman, E., Lipton, S. A., and Loring, R. H. (1989) Selective modulation of NMDA responses by reduction and oxidation, *Neuron 2*, 1257−1263.
43. Mendieta, J., Ramirez, G., and Gago, F. (2001) Molecular dynamics simulations of the conformational changes of the glutamate receptor ligand-binding core in the presence of glutamate and kainate, *Proteins: Struct., Funct., Genet. 44*, 460−469.
44. Arinaminpathy, Y., Sansom, M. S. P., and Biggin, P. C. (2002) Molecular dynamics simulations of the ligand-binding domain of the ionotropic glutamate receptor GluR2, *Biophys. J. 82*, 676−683.
45. Kubo, M., Shiomitsu, E., Odai, K., Sugimoto, T., Suzuki, H., and Ito, E. (2003) Agonist-specific vibrational excitation of glutamate receptor, *J. Mol. Struct. 639*, 117−128.
46. Kubo, M., Shiomitsu, E., Odai, K., Sugimoto, T., Suzuki, H., and Ito, E. (2004) Picosecond dynamics of the glutamate receptor in response to agonist induced vibrational excitation, *Proteins: Struct., Funct., Genet. 54*, 231−236.
47. Speranskiy, K., and Kurnikova, M. (2005) On the binding determinants of the glutamate agonist with the glutamate receptor ligand binding domain, *Biochemistry 44*, 11508−11517.
48. Mamonova, T., Hespenheide, B., Straub, R., Thorpe, M. F., and Kurnikova, M. (2005) Protein flexibility using constraints from molecular dynamics simulations, *Phys. Biol. 2*.
49. Mendieta, J., Gago, F., and Ramirez, G. (2005) Binding of 5′-GMP to the GluR2 AMPA receptor: insight from targeted molecular dynamics simulations, *Biochemistry 44*, 14470−14476.
50. Arinaminpathy, Y., Sansom, M. S. P., and Biggin, P. C. (2006) Binding site flexibility: Molecular simulation of partial and full agonists within a glutamate receptor, *Mol. Pharmacol. 69*, 11−18.
51. Pentikainen, U., Settimo, L., Johnson, M. S., and Pentikainen, O. T. (2006) Subtype selectivity and flexibility of ionotropic glutamate receptors upon antagonist ligand binding, *Org. Biomol. Chem. 4*, 1058−1070.
52. Sanders, J. M., Pentikäinen, O. T., Settimo, L., Pentikäinen, U., Shoji, M., Sasaki, M., Sakai, R., Johnson, M. S., and Swanson, G. T. (2006) Determination of binding site residues responsible for the subunit selectivity of novel marine-derived compounds on kainate receptors, *Mol. Pharmacol. 69*, 1849−1860.
53. Chen, P. E., Geballe, M. T., Stansfeld, P. J., Johnston, A. R., Yuan, H., Jacob, A. L., Snyder, J. P., Traynelis, S. F., and Wyllie, D. J. A. (2005) Structural features of the glutamate binding site in recombinant NR1/NR2A *N*-methyl-D-aspartate receptors determined by site-directed mutagenesis and molecular modeling, *Mol. Pharmacol. 67*, 1471−1484.
54. Kaye, L. S., Sansom, M. S. P., and Biggin, P. C. (2006) Molecular dynamics simulations of an NMDA receptor, *J. Biol. Chem. 281*, 12736−12742.
55. Kubo, M., and Ito, E. (2004) Structural dynamics of an ionotropic glutamate receptor, *Proteins: Struct., Funct., Bioinf. 56*, 411−419.
56. Fiser, A., and Sali, A. (2003) Modeller: generation and refinement of homology-based protein structure models, *Methods Enzymol. 374*, 461−491.
57. Hermans, J., Berendsen, H. J. C., van Gunsteren, W. F., and Postma, J. P. M. (1984) A consistent empirical potential for water-protein interactions, *Biopolymers 23*, 1513−1518.

58. Berendsen, H. J. C., van der Spoel, D., and van Drunen, R. (1995) GROMACS: A message-passing parallel molecular dynamics implementation, *Comput. Phys. Commun. 95*, 43−56.
59. Lindahl, E., Hess, B., and van der Spoel, D. (2001) GROMACS 3.0: A package for molecular simulation and trajectory analysis, *J. Mol. Model. 7*, 306−317.
60. Berendsen, H. J. C., Postma, J. P. M., van Gunsteren, W. F., DiNola, A., and Haak, J. R. (1984) Molecular dynamics with coupling to an external bath, *J. Chem. Phys. 81*, 3684−3690.
61. Oostenbrink, C., Villa, A., Mark, A. E., and Van Gunsteren, W. F. (2004) A biomolecular force-field based on the free enthalpy of hydration and solvation. The GROMOS force-field parameter sets 53A5 and 53A6, *J. Comput. Chem. 25*, 1656−1676.
62. Darden, T., York, D., and Pedersen, L. (1993) Particle mesh Ewald−an N.log(N) method for Ewald sums in large systems, *J. Chem. Phys. 98*, 10089−10092.
63. Essman, U., Perera, L., Berkowitz, M. L., Darden, T., Lee, H., and Pedersen, L. G. (1995) A smooth particle mesh Ewald method, *J. Chem. Phys. 103*, 8577−8593.
64. Hess, B., Bekker, J., Berendsen, H. J. C., and Fraaije, J. G. E. M. (1997) LINCS: A linear constraint solver for molecular simulations, *J. Comput. Chem. 18*, 1463−1472.
65. Kabsch, W., and Sander, C. (1983) Dictionary of protein secondary structure: pattern recognition of hydrogen-bonded and geometrical features, *Biopolymers 22*, 2577−2637.
66. Mayer, M. L., Ghosal, A., Dolman, N. P., and Jane, D. E. (2006) Crystal structures of the kainate receptor GluR5 ligand binding core dimer with novel GluR5-selective antagonists, *J. Neurosci. 26*, 2852−2861.
67. Ramanoudjame, G., Mei, D., Mankiewicz, K. A., and Jayaraman, V. (2006) Allosteric mechanism in AMPA receptors: A FRET-based investigation of conformational changes, *Proc. Natl. Acad. Sci. U.S.A. 103*, 10473−10478.
68. Madden, D. R., Armstrong, N., Svergun, D., Perez, J., and Vachette, P. (2005) Solution X-ray scattering evidence for agonist and antagonist induced modulation of cleft closure in a glutamate receptor ligand-binding domain, *J. Biol. Chem. 280*, 23737−23642.
69. Mayer, M. L., Olson, R., and Gouaux, E. (2001) Mechanisms for ligand binding to GluR0 ion channels: Crystal structures of the glutamate and serine complexes and a closed apo state, *J. Mol. Biol. 311*, 815−836.
70. Ghezzi, P. (2005) Oxidoreduction of protein thiols in redox regulation, *Biochem. Soc. Trans. 33*, 1378−1381.
71. Pang, A., Arinaminpathy, Y., Sansom, M. S. P., and Biggin, P. C. (2005) Comparative molecular dynamics: Similar folds and similar motions?, *Proteins: Struct., Funct., Bioinf. 61*, 809−822.
72. Valentine, E. R., and Palmer, A. G., III (2005) Microsecond-to-millisecond conformational dynamics demarcate the GluR2 glutamate receptor bound to agonists glutamate, quisqualate and AMPA, *Biochemistry 44*, 3410−3417.
73. McFeeters, R. L., and Oswald, R. E. (2002) Structural mobility of the extracellular ligand-binding core of an ionotropic glutamate receptor. Analysis of NMR relaxation dynamics, *Biochemistry 41*, 10472−10481.
74. Colquhoun, D. (1998) Binding, gating, affinity and efficacy: The interpretation of structure-activity relationships for agonists and of the effects of mutating receptors, *Br. J. Pharmacol. 125*, 923−947.
75. Regalado, M. P., Villarroel, A., and Lerma, J. (2001) Intersubunit cooperativity in the NMDA receptor, *Neuron 32*, 1085−1096.
76. Popescu, G. (2005) Principles of *N*-methyl-D-aspartate receptor allosteric modulation, *Mol. Pharmacol. 68*, 1148−1155.

BI061462D